ORIGINAL PAPER

Ethylene Epoxidation in Low-Temperature AC Dielectric Barrier Discharge: Effects of Oxygen-to-Ethylene Feed Molar Ratio and Operating Parameters

Thammanoon Sreethawong · Thanapoom Suwannabart · Sumaeth Chavadej

Abstract Ethylene oxide (EO), a valuable chemical feedstock in producing many industrial chemicals, which is industrially produced by the partial oxidation of ethylene, so-called ethylene epoxidation, has been of great interest in many global research studies. In this work, the epoxidation of ethylene under a low-temperature dielectric barrier discharge (DBD) was feasibly investigated to find the best operating conditions. It was experimentally found that the EO yield decreased with increasing O_2/C_2H_4 feed molar ratio, feed flow rate, input frequency, and electrode gap distance, while it increased with increasing applied voltage up to 19 kV. The highest EO yield of 5.6% was obtained when an input frequency of 500 Hz and an applied voltage of 19 kV were used, with an O_2/C_2H_4 feed molar ratio of 1:1, a feed flow rate of 50 cm³/min, and an electrode gap distance of 10 mm. Under these best conditions, the power consumption was found to be as low as 6.07×10^{-16} Ws/molecule of EO produced.

Introduction

Ethylene oxide (C_2H_4O, EO) is an important industrial chemical, which is primarily used as an intermediate in the production of various useful chemicals. Its major use is in the production of ethylene glycol. It is also used for the manufacture of surfactants and detergents by a process called ethoxylation, solvents, antifreezes, adhesives, polyurethane foam, fumigants for agricultural products, and sterilants for medical equipment and supplies, spices, and cosmetics [1, 2]. Since EO is a valuable chemical feedstock for many

T. Sreethawong · T. Suwannabart · S. Chavadej (✉)
The Petroleum and Petrochemical College, Chulalongkorn University, Soi Chula 12, Phyathai Road, Pathumwan, Bangkok 10330, Thailand
e-mail: sumaeth.c@chula.ac.th

applications, the selective partial oxidation of ethylene to EO, so-called ethylene epoxidation, has been of great interest in global research works.

As discovered by Lefort in 1931 [3], the gas phase epoxidation of ethylene to EO using molecular oxygen and silver catalysts is one of the greatest findings in heterogeneous catalysis, being the most widely used method for ethylene epoxidation. Since 1940, almost all EO produced industrially has been made using this method [4]. To date, silver catalysts supported on alpha-alumina (Ag/α-Al$_2$O$_3$) with alkali and transition metal promoters [5–15], such as Cs, Cu, Re, and Au, or with addition of chlorine-containing moderators into gaseous reactants [16–20], such as dichloroethane (C$_2$H$_4$Cl$_2$) and vinyl chloride (C$_2$H$_3$Cl), provide high selectivity for EO. However, the conventional catalytic process normally requires high temperatures, i.e. implying high energy consumption, to sufficiently activate the catalyst for the ethylene epoxidation, basically higher than 200°C. Moreover, the catalytic problems at high temperature operation, i.e. catalyst deactivation, catalyst regeneration, and catalyst replacement, greatly reduces the working efficiency of the process, as well as directly leads to a high production cost. These turn out to become necessary for developing a new approach to overcome the mentioned problems.

Non-thermal plasmas, such as dielectric barrier discharge (DBD), corona discharge, and glow discharge, are a highly potential alternative for chemical reaction investigation under non-equilibrium conditions operated at low temperatures and atmospheric pressure. The main characteristic of the non-equilibrium plasma is its high electron temperatures (10^4–10^5 K), whereas the bulk gas temperature remains as low as room temperature [21, 22]. This implies comparatively lower energy consumption used for operating the reaction system as compared with conventional catalytic processes. The non-equilibrium plasma with the highly energetic electrons and low temperature in the bulk gas can initiate several chemical reactions, which are normally not possible to occur at low temperatures [23].

DBD is the most commonly used technique for atmospheric pressure plasma operation. The basic principle of this technique is to utilize non-equilibrium plasma, in which the major part of electrical energy is transferred to energetic electrons and active radical species generated from subsequent reactions [24]. A major advantage of DBD is that the entire electrode area is effectively employed for discharge generation, resulting in the comparatively high discharge volume with a very low temperature typically close to room temperature. The uses of DBD for chemical syntheses and conversions have become increasingly important for several applications, such as the partial oxidation of methane to methanol [24], the ozone production from molecular oxygen [25], the removal of gaseous H$_2$S and NH$_3$ [26], the oxidation of propene [27], the decomposition of trichloroethylene [28], the reforming of hydrocarbons and alcohols for hydrogen production [29], and the methane conversion to C$_2$ hydrocarbons [30]. However, up to now, the use of DBD for gas phase epoxidation reaction has been rarely investigated. To our knowledge, only one recent published work described about gas phase epoxidation of propylene [31]; however, there has been no any literature reporting the epoxidation of ethylene using DBD yet.

In this work, a low-temperature DBD system was employed for the first time for non-catalytic ethylene epoxidation at atmospheric pressure. The effects of various operating parameters, including O$_2$/C$_2$H$_4$ feed molar ratio, feed flow rate, input frequency, applied voltage, and electrode gap distance, on the activity of ethylene epoxidation and the system performance were extensively examined.

Experimental

Reactant Gases

All gases used in this work, i.e. 99.995% helium (high purity grade), 40% ethylene balanced with helium, and 97% oxygen balanced with helium, were supplied by Thai Industrial Gas (Public) Co., Ltd.

Dielectric Barrier Discharge System

The experimental study of ethylene epoxidation was conducted in a low-temperature DBD system, which was operated at atmospheric pressure and ambient temperature, around 25–27°C (room temperature). The schematic of the DBD system is shown in Fig. 1a. The acrylic plate-made DBD reactor sizes were 2 cm height × 3 cm width × 15 cm length for the inner dimensions, and 3 cm height × 7 cm width × 19 cm length for the outer dimensions. As shown in Fig. 1b, it consists of a 5-mm-thick dielectric glass plate placed between two parallel stainless steel electrodes, on the lower electrode. The gap distance between the electrodes was varied from 10 to 14 mm. The input power used to generate
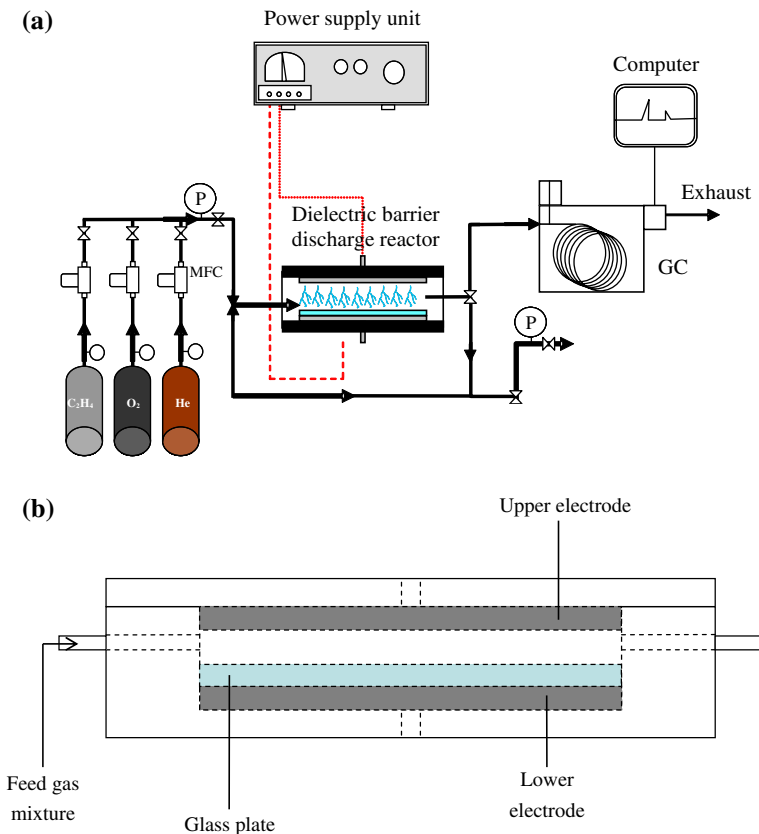

Fig. 1 (**a**) Schematic of experimental setup for ethylene epoxidation reaction in dielectric barrier discharge plasma system and (**b**) configuration of the dielectric barrier discharge reactor

microdischarge plasma between the electrode gap was domestic alternating current (AC), 200 V and 50 Hz, which was transmitted to a high voltage current via a power supply unit. The power supply unit consisted of three steps. For the first step, the domestic AC input of 220 V and 50 Hz was converted to a DC output of 70 V by a DC power supply converter. For the second step, a 500 W power amplifier with a function generator was used to transform the DC into AC current with a sinusoidal waveform and different frequencies. For the third step, the outlet voltage was stepped up by using a high voltage transformer. The description of the power supply unit was given elsewhere [32]. The output voltage and frequency were controlled by the function generator. The voltage and current at the low voltage side were measured instead of those at the high voltage side across the electrodes since the plasma generated is non-equilibrium in nature. The high side voltage and current were thereby calculated by multiplying and dividing by a factor of 130, respectively [32–35]. A power analyzer was used to measure power, current, frequency, and voltage at the low voltage side of the power supply unit.

Reaction Testing Procedure

Reactant gases (ethylene, oxygen, and helium) fed through the plasma reactor were controlled by a set of electronic mass flow controllers and transducers, supplied by SIERRA® Instrument Inc., to obtain a feed gas mixture having different flow rates and oxygen-to-ethylene molar ratios. A 7-μm in-line filter was placed upstream of each mass flow controller in order to trap any solid particles. A check valve was placed downstream of each mass flow controller to prevent any back flow of the reactant gases. All of the reactant gases were mixed inside a single line before being introduced into the DBD reactor. For any studied conditions, the feed gas mixture was first introduced into the DBD system without turning on the power supply unit. After the composition of outlet gas was invariant with time, it was turned on. The outlet of the reactor was either vented to the atmosphere via rubber tube exhaust or was connected to an on-line gas chromatograph (Perkin–Elmer, AutoSystem GC) for analysis of the product gases. The moisture in the product gas stream was trapped by a water trap filter before entering a heated stainless steel line to the on-line gas chromatograph. The gas chromatograph was equipped with both a thermal conductivity detector (TCD) and a flame ionization detector (FID). For the TCD channel, the packed column (Carboxen 1000) was used for separating the product gases, which were hydrogen (H_2), oxygen (O_2), carbon monoxide (CO), carbon dioxide (CO_2), and ethylene (C_2H_4). For the FID channel, the capillary column (OV-Plot U) was used for analysis of EO and other by-product gases, i.e. CH_4, C_2H_2, C_2H_6, and C_3H_8. The composition of product gas stream was analyzed by the on-line gas chromatograph every 20 min. After the system reached steady state, an analysis of outlet gas composition was taken at least a few times. The experimental data taken under steady state conditions were averaged, and these averages were used to evaluate the performance of the plasma system. It is also worth noting that during the reaction, the temperature at the reactor wall was found to be lower than the melting temperature of acrylic plate (130°C), which was used to construct the DBD reactor.

Reaction Performance Assessment

To evaluate the process performance, the conversions of ethylene and oxygen and the selectivities for products, including EO, CO, CO_2, H_2, CH_4, C_2H_2, C_2H_6, and traces of C_3, were considered. The conversion of either ethylene or oxygen is defined as:

$$\% \text{ Reactant conversion} = \frac{(\text{moles of reactant } in - \text{moles of reactant } out)(100)}{(\text{moles of reactant } in)}$$

The product selectivity is calculated from the following equation:

$\%$ Product selectivity

$$= \frac{[(\text{number of carbon or hydrogen atom in product}) \, (\text{moles of product produced})](100)}{[(\text{number of carbon or hydrogen atom in ethylene})(\text{moles of ethylene converted})]}$$

The EO yield is calculated from the following equation:

$$\% \text{ EO yield } = (\% \text{ ethylene conversion}) \, (\% \text{ EO selectivity}) \, (100)$$

To determine the energy efficiency of the plasma system, the specific power consumption is calculated in a unit of Ws per molecule of converted ethylene or per molecule of produced EO using the following equation:

$$\text{Specific power consumption} = \frac{(P)(60)}{(N)(M)}$$

where $P = \text{Power (W)}$, $N = \text{Avogadro's number} = 6.02 \times 10^{23} \text{ molecules/mol}$, $M = \text{Rate}$ of converted ethylene molecules in feed or rate of produced EO molecules (mol/min).

Results and Discussion

Effect of Feed Molar Ratio of O_2/C_2H_4

The effect of O_2/C_2H_4 feed molar ratio was initially studied in order to obtain the most suitable feed gas composition for ethylene epoxidation reaction under the low-temperature DBD system. In this study, the O_2/C_2H_4 feed molar ratio was investigated in the range of 1:1–4:1, while an applied voltage of 17 kV, an input frequency of 550 Hz, and a residence time of 0.45 min were used as base conditions to operate the DBD system. The residence time is calculated by the inside volume of the DBD reactor divided by a feed flow rate. The effect of O_2/C_2H_4 feed molar ratio on the C_2H_4 and O_2 conversions and the EO yield is shown in Fig. 2a, and that on the selectivities for EO, CO, CO_2, H_2, CH_4, C_2H_2, C_2H_6, and C_3H_8 is shown in Fig. 2b. The increase in the O_2/C_2H_4 feed molar ratio slightly affected the reactant conversions, but it mainly affected the EO and CO_2 selectivities, especially in the O_2/C_2H_4 feed molar ratio range between 1:1 and 3:1. This can be explained in that a higher O_2/C_2H_4 feed molar ratio leads to more O_2 content available to react with various hydrocarbon molecules, as well as EO and CO, to convert to CO_2. However, the conversion of O_2 reached a maximum in the O_2/C_2H_4 feed molar ratio range between 2:1 and 3:1, which is about the theoretical ratio for C_2H_4 complete combustion, as shown in the following equation. At a feed molar ratio higher than 3:1 or excess O_2 condition, the conversion of O_2 tended to decrease since O_2 is probably consumed at the same level.

$$C_2H_4 + 3O_2 \rightarrow 2CO_2 + 2H_2O$$
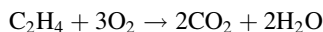
For the DBD system operated under the studied conditions, the yield of EO and the selectivities for EO, H_2, C_2H_2, and C_2H_6 tended to decrease, but in contrast, the selectivity for CO_2 increased with increasing O_2/C_2H_4 feed molar ratio, as aforementioned.
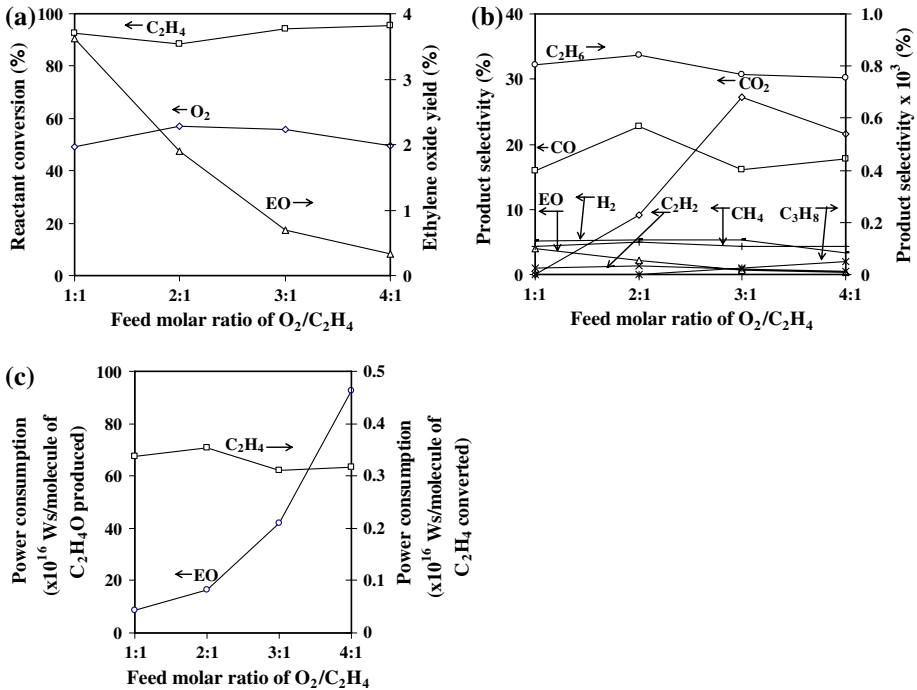
Fig. 2 (**a**) Conversions of ethylene and oxygen and yield of EO, (**b**) product selectivities, and (**c**) power consumptions as a function of O_2/C_2H_4 feed molar ratio (feed flow rate = 50 cm³/min; electrode gap distance = 10 mm; applied voltage = 17 kV; input frequency = 550 Hz; and residence time = 0.45 min)

Interestingly, the selectivity for CH_4 remained almost constant in the studied range of O_2/C_2H_4 feed molar ratio. The CO selectivity increased when the O_2/C_2H_4 feed molar ratio increased, and it reached a maximum at the O_2/C_2H_4 feed molar ratio of 2:1. Beyond the O_2/C_2H_4 feed molar ratio of 2:1, the CO selectivity decreased and reached a plateau at the theoretical O_2/C_2H_4 feed molar ratio for complete combustion of 3:1. Under the studied conditions, the main products were CO and CO_2 with significant amounts of EO, H_2, CH_4, and C_2 products (C_2H_2 and C_2H_6). The highest hydrocarbon, i.e. C_3H_8, was found in a very small fraction. The results can be explained by the fact that under the presence of oxygen, both complete and partial oxidation reactions are dominant. The decrease in the selectivities for these hydrocarbons and H_2 and the increase in the selectivity for CO_2 with increasing oxygen fraction in feed clearly reveal that the oxidative dehydrogenation and coupling reactions unfavorably occurred under O_2-rich conditions, as expected. The EO selectivity was found to be the highest at the O_2/C_2H_4 feed molar ratio of 1:1 and decreased with increasing O_2/C_2H_4 feed molar ratio. Furthermore, at a very high O_2/C_2H_4 feed molar ratio of 4:1, the selectivity for EO dropped to zero level since this high O_2/C_2H_4 feed molar ratio induced the complete combustion to occur more favorably than the partial oxidation, as well as the epoxidation, indicating that the epoxidation reaction to produce EO is more likely to occur under O_2-lean conditions.

Figure 2c shows the power consumptions used to convert an ethylene molecule and to produce an EO molecule at different O_2/C_2H_4 feed molar ratios. The power consumption per molecule of converted ethylene reached a maximum when the O_2/C_2H_4 feed molar

ratio increased up to 2:1 and slightly decreased with further increasing feed molar ratio. However, there was a significant increase in the power consumption per molecule of produced EO with increasing O_2/C_2H_4 feed molar ratio, especially at the feed molar ratio higher than 3:1. It is also worth noting that the power consumption per molecule of EO produced was approximately two orders of magnitude higher than that per molecule of ethylene converted. Hence, an O_2/C_2H_4 feed molar ratio of 1:1 was therefore selected for further investigation because it provided the highest selectivity and yield for EO and the lowest power consumption per molecule of EO produced.

Effect of Feed Flow Rate

The feed flow rate plays a significant role on the residence time of gas molecules within the plasma zone, affecting the performance of the plasma system. The experiments were performed by varying feed flow rate from 50 to 75, 100, and 125 cm^3/min, corresponding to the residence time of 0.45, 0.3, 0.225, and 0.18 min, respectively. At a feed flow rate lower than 50 cm^3/min, the O_2 flow rate cannot be adjusted due to the limitation of a mass flow controller. The studied plasma system was operated at an O_2/C_2H_4 feed molar ratio of 1:1, an applied voltage of 17 kV, and an input frequency of 550 Hz. Figure 3a illustrates the influences of the feed flow rate on the C_2H_4 and O_2 conversions. The conversion of O_2 gradually decreased with increasing the feed flow rate from 50 to 125 cm^3/min while the conversion of C_2H_4 more sharply decreased. An increase in the feed flow rate generally reduces the gas residence time in the reaction system, resulting in having a shorter contact time of ethylene and oxygen molecules to collide with electrons. As a result, a reduction in the feed flow rate enhances the conversions of both C_2H_4 and O_2, which leads to an increase in the yield of EO, as also shown in Fig. 3a.

The feed flow rate dependence of product selectivities is depicted in Fig. 3b. It is apparent that increasing feed flow rate predominantly resulted in decreases in the selectivities for EO and CO. This is because a higher feed flow rate reduces the opportunity of collision between electrons/oxygen active species and reactant/intermediate molecules to render the partial oxidation and epoxidation reactions. But for other products, especially C_2H_2 and C_3H_8, their selectivities tended to increase at shorter residence times due to higher feed flow rates, suggesting that the oxidative dehydrogenation and coupling reaction are more favorable to occur than the partial oxidation when the residence time is decreased.

Figure 3c shows the effect of feed flow rate on the power consumptions. The power consumption per molecule of converted ethylene slightly decreased, but the power consumption per molecule of produced EO tended to greatly increase with increasing feed flow rate. The lower feed flow rate gave comparatively low power consumption per molecule of produced EO, as well as much higher reactant conversions and desired product selectivity. Therefore, the feed flow rate of 50 cm^3/min was selected as a best condition and used for further investigation.

Effect of Input Frequency

Input frequency is one of the most important parameters in plasma reactor operation, significantly affecting the field strength in the plasma zone. The studied DBD system was operated in the frequency range of 500–800 Hz. At a frequency lower than 500 Hz, the plasma distribution was not fairly uniform over the whole electrode surface, and it tended to appear as a single strong stream of plasma discharge, whereas the plasma could not exist
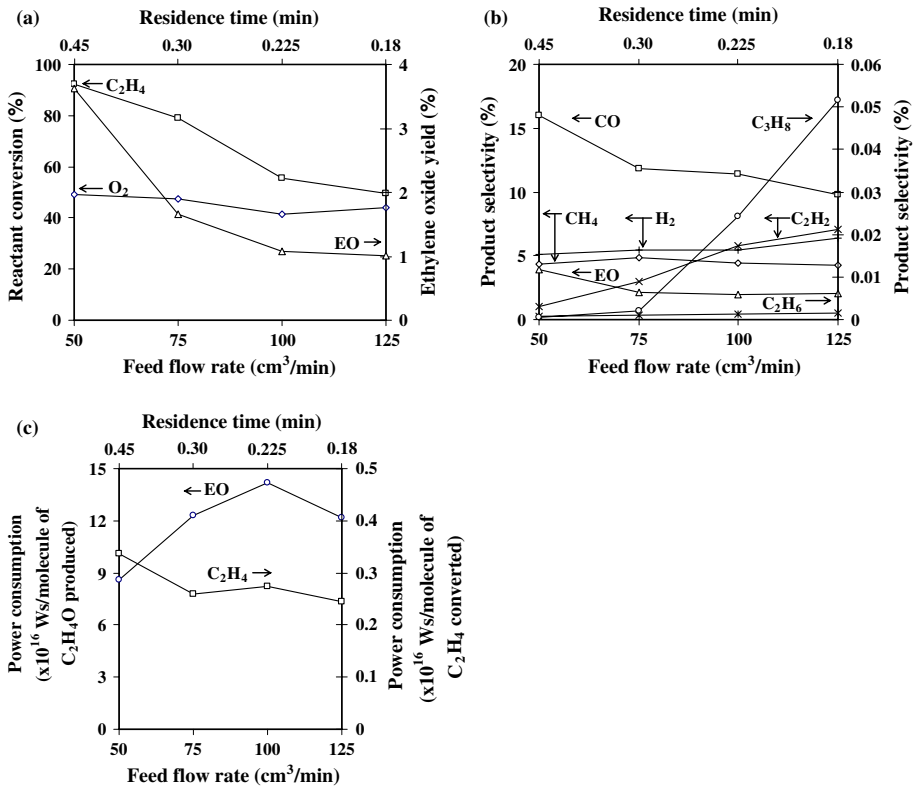
Fig. 3 (a) Conversions of ethylene and oxygen and yield of EO, (b) product selectivities, and (c) power consumptions as a function of feed flow rate (feed molar ratio of $O_2/C_2H_4 = 1:1$; electrode gap distance = 10 mm, applied voltage = 17 kV, and input frequency = 550 Hz)

at a frequency higher than 800 Hz. The effect of input frequency on the C_2H_4 and O_2 conversions and the yield of EO is illustrated in Fig. 4a. When the input frequency was increased in the range of 500–650 Hz, the O_2 and C_2H_4 conversions and EO yield decreased dramatically, and they turned to slightly decrease with further increasing input frequency from 650 up to 800 Hz. The explanation is that a higher frequency results in a lower current that corresponds to the reduction of the number of electrons generated (weaker field strength), as shown in Fig. 4b. It therefore causes the decrease in amount of active species for further reactions, resulting in the decrease in the C_2H_4 and O_2 conversions and subsequently leading to the lower yield of EO.

The effect of input frequency on the product selectivities is shown in Fig. 4c. The selectivities for EO and CO tended to slightly decrease with increasing input frequency up to 650 Hz. At a higher frequency than 650 Hz, the partial oxidation, oxidative dehydrogenation, and coupling reactions to form various products increasingly occurred. Beyond 650 Hz, the selectivity for EO also gradually increased with increasing frequency and reached a maximum of 7.3% at 800 Hz, as compared with 5.0% at 500 Hz for the low frequency range between 500 and 650 Hz. However, the input frequency of 500 Hz was considered as a potentially best value, exhibiting the highest EO yield with a reasonably high EO selectivity and a relatively low CO selectivity.
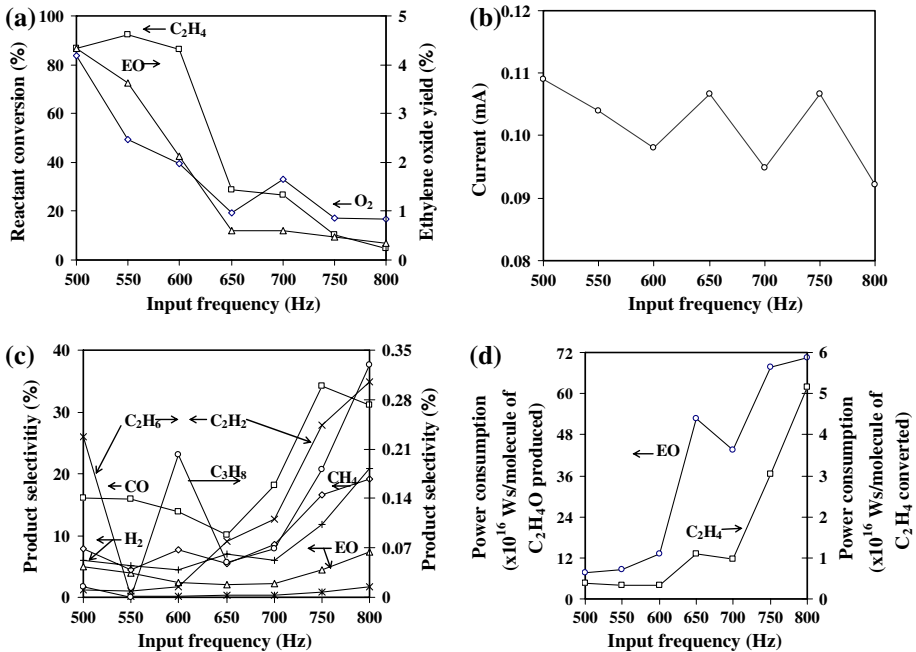
Fig. 4 (**a**) Conversions of ethylene and oxygen and yield of EO, (**b**) generated current, (**c**) product selectivities, and (**d**) power consumptions as a function of input frequency (feed molar ratio of O_2/C_2H_4 = 1:1; feed flow rate = 50 cm^3/min; electrode gap distance = 10 mm; applied voltage = 17 kV; and residence time = 0.45 min)

The effect of input frequency on the power consumptions to break down each C_2H_4 molecule and to create each EO molecule is shown in Fig. 4d. The results showed that both the power consumptions per C_2H_4 molecule converted and per EO molecule produced tended to increase with increasing input frequency, especially at an input frequency higher than 600 Hz. Based upon the relatively high EO yield and the lowest power consumption per molecule of EO produced, the best input frequency of 500 Hz was selected for further investigation.

Effect of Applied Voltage

Under the studied conditions, the break-down voltage or the lowest voltage to generate plasma (onset voltage) was found to be about 13 kV, and the DBD system could not be operated at the applied voltage higher than 21 kV since the generated plasma was found to have the non-uniform distribution characteristic. Therefore, the reaction experiments were conducted in the voltage range of 13–21 kV in order to determine the effect of the applied voltage. The effect of applied voltage on the C_2H_4 and O_2 conversions and EO yield is illustrated in Fig. 5a. The oxygen conversion and EO yield tended to considerably increase with increasing applied voltage in the range of 13–19 kV, whereas the ethylene conversion slightly increased. With further increasing applied voltage higher than 19 kV, the reactant conversions and the EO yield did not significantly change. The explanation for the rapid increment in the O_2 conversion with increasing applied voltage is that a higher voltage results in a higher current (stronger field strength), as shown in Fig. 5b, leading to more
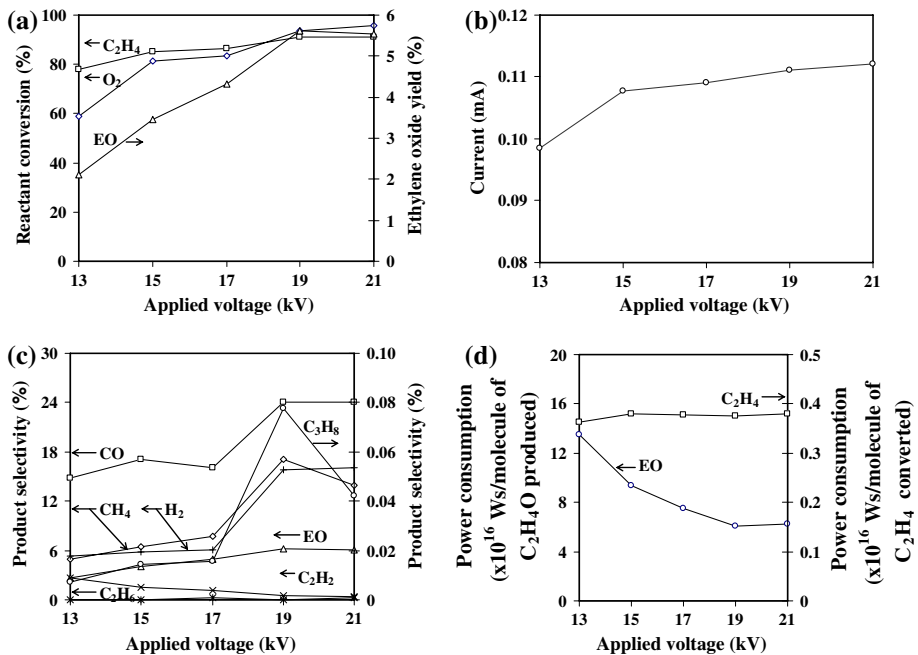
Fig. 5 (**a**) Conversions of ethylene and oxygen and yield of EO, (**b**) generated current, (**c**) product selectivities, and (**d**) power consumptions as a function of applied voltage (feed molar ratio of O_2/C_2H_4 = 1:1; feed flow rate = 50 cm³/min; electrode gap distance = 10 mm; input frequency = 500 Hz; and residence time = 0.45 min)

available electrons to increase an opportunity for collision with oxygen. The results correspond well with the previous works [32–37]. In contrast, it is unexpected that the C_2H_4 conversion only slightly increased with increasing applied voltage. This can be explained in that the bond dissociation energy of C_2H_4 (16.7 eV) is much higher than that of O_2 (12.2 eV), particularly causing O_2 molecules to be converted more easily than C_2H_4.

The effect of applied voltage on the selectivities for EO, CO, H_2, CH_4, C_2H_2, C_2H_6, and C_3H_8 is shown in Fig. 5c. The selectivities for EO, CO, H_2, and other hydrocarbon products, except C_2H_2 selectivity, increased with increasing applied voltage. When the applied voltage increased, corresponding to increasing O active species as mentioned above, C_2H_4 and other hydrocarbons are easily oxidized to form more CO and EO. Interestingly, no CO_2 was detected under the studied conditions since the system was operated under the O_2-lean condition (the O_2/C_2H_4 feed molar ratio of 1:1). The results therefore suggest that a higher applied voltage is more favorable for EO production under the O_2-lean condition. Only the selectivity for C_2H_2 was observed to decrease with increasing applied voltage. This might be because the formed C_2H_2 further reacts with largely available O active species to form other products more easily. Interestingly, the further increase in applied voltage higher than 19 kV did not help enhance the EO production.

Figure 5d shows the effect of applied voltage on the power consumptions. With increasing applied voltage, the power consumption per molecule of converted C_2H_4 remained almost unchanged, whereas the power consumption per molecule of produced EO substantially decreased. As mentioned earlier, the slight increase in ethylene

conversion with increasing applied voltage caused insignificant change in the power consumption per molecule of ethylene converted. In contrast, an increase in the selectivity for EO was comparatively high as increasing applied voltage, resulting in lower power consumption per molecule of produced EO.

From the results, the applied voltage of 19 kV was selected to be the best value because this voltage provided the reasonably high conversions of C_2H_4 and O_2, and the highest selectivity and yield for EO. At a higher voltage, it did not affect any of reactant conversion, EO selectivity, and EO yield. Moreover, at the applied voltage of 19 kV, the lowest power consumption per EO molecule produced was obtained.

Effect of Electrode Gap Distance

The effects of electrode gap distance and corresponding residence time have been shown to be very important in plasma system operation [35, 37–39]. The effect of electrode gap distance was studied under the best conditions achieved above; an O_2/C_2H_4 feed molar ratio of 1:1, a feed flow rate of 50 cm^3/min, an input frequency of 500 Hz, and an applied voltage of 19 kV. The electrode gap distance was varied from 10 to 11, 12, 13, and 14 nm, corresponding to the residence time of 0.45, 0.54, 0.63, 0.72, and 0.81 min, respectively. The lowest electrode gap distance for the studied DBD system was limited at 10 mm due to its configuration. At an electrode gap distance higher than 14 mm, the generated plasma became unfavorably non-uniform. Therefore, the reaction experiments were conducted in the range of electrode gap distance between 10 and 14 mm in order to determine the effect of the electrode gap distance.

The effect of electrode gap distance on the C_2H_4 and O_2 conversions and EO yield is illustrated in Fig. 6a. The ethylene conversion and EO yield tended to decrease with increasing the electrode gap distance, whereas the oxygen conversion tended to be almost unchanged. The explanation for slight ethylene conversion decrement is that a wider electrode gap distance results in a higher residence time for several hydrocarbon species to recombine via coupling reactions, including backward reaction to form ethylene, causing lower conversion of ethylene. The unexpected nearly constant O_2 conversion with increasing electrode gap distance can be explained in that the current slightly increases with increasing electrode gap distance, as shown in Fig. 6b, while the residence time is also increased. The results suggest that for the O_2 conversion, the higher probability in converting O_2 molecules due to higher electron density might trade off the higher probability in oxygen active species recombination due to a longer residence time of gas flow. The expected increase in current, i.e. electron density, might be contributed to the special characteristic of the DBD system containing the dielectric plate, as well as the various compositions of gaseous species inside the plasma zone. At a higher electrode gap distance, the dielectric plate might sustain the discharge a little bit more effectively due to less loss of electrons via various reactions, under the identical input frequency and applied voltage.

The effect of electrode gap distance on the selectivities for EO, CO, H_2, CH_4, C_2H_2, C_2H_6, and C_3H_8 is shown in Fig. 6c. The selectivities for EO, CO, H_2, and CH_4 decreased with increasing gap distance while the opposite trend was observed for C_2H_2, C_2H_6, and C_3H_8. These may be implied that when increasing electrode gap distance, the opportunity of coupling reactions more favorably occur as secondary reactions than the partial oxidation, as above explained.

Figure 6d shows the effect of electrode gap distance on the power consumptions. It is clearly seen that both the power consumptions per molecule of converted C_2H_4 conversion
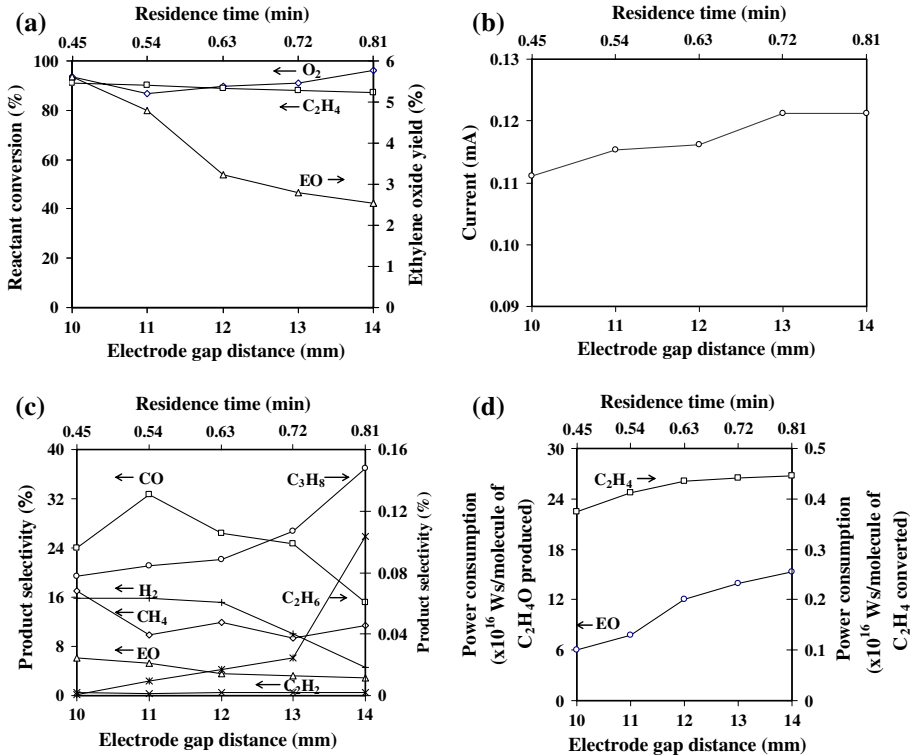
Fig. 6 (**a**) Conversions of ethylene and oxygen and yield of EO, (**b**) generated current, (**c**) product selectivities, and (**d**) power consumptions as a function of electrode gap distance (feed molar ratio of O_2/C_2H_4 = 1:1; feed flow rate = 50 cm^3/min; applied voltage = 19 kV; and input frequency = 500 Hz)

and per molecule of produced EO substantially increased with increasing electrode gap distance. A higher electrode gap distance causes a higher probability of secondary reactions, which unavoidably uses up some power. From the results, the electrode gap distance of 10 mm was considered as a best value because at 10 mm gap distance, the highest EO selectivity and EO yield with the lowest power consumption per EO molecule produced were achieved.

In comparisons, although the maximum EO yield of 5.6% obtained under the aforementioned best conditions (an O_2/C_2H_4 feed molar ratio of 1:1, a feed flow rate of 50 cm^3/min, an input frequency of 500 Hz, an applied voltage of 19 kV, and an electrode gap distance of 10 mm) using the studied DBD system was lower than the EO yields of 30 and 10% obtained from the catalytic epoxidation process using 15 wt.% Ag/Al_2O_3 at reaction temperatures of 280 and 350°C, respectively [15], the DBD system is still considered to exhibit a high potential to be employed for EO production under much lower operating temperatures. Again, the present work is the first time to demonstrate the use of the sole DBD system to synthesize EO without the presence of catalysts. As shown in the aforementioned results, there were several reactions occurring in the plasma reaction zone so it is not possible to easily carry out the kinetic consideration of the ethylene epoxidation reaction. Future works will then be focused on the combination of the low-temperature DBD system with various reported catalytically active catalysts used in the conventional catalytic process, especially Ag/Al_2O_3-based catalysts [5–15, 20], aiming to enhance the

EO yield. The comparative study of ethylene epoxidation under different kinds of low-temperature plasma discharges, such as corona discharge system with pin and plate electrodes, is also of our strong interest. Moreover, the kinetic studies of the ethylene epoxidation reaction will be conducted in order to optimize the DBD process. The experimental results will be presented in the next contribution.

Conclusions

In this work, the epoxidation reaction of ethylene was investigated in the low-temperature DBD plasma system. The effects of various operating parameters, including feed molar ratio of O_2/C_2H_4, feed flow rate, input frequency, applied voltage, and electrode gap distance, on the ethylene epoxidation reaction was studied in order to achieve the best conditions. In order to obtain the highest EO yield of 5.6% and the highest selectivity of 6.2%, the DBD system must be operated at an O_2/C_2H_4 feed molar ratio of 1:1, a feed flow rate of 50 cm^3/min, an input frequency of 500 Hz, an applied voltage of 19 kV, and an electrode gap distance of 10 mm. At these best conditions, the power consumptions to break down each C_2H_4 molecule and to create EO molecule were found to be 0.37×10^{-16} Ws/molecule of C_2H_4 converted and 6.07×10^{-16} Ws/molecule of EO produced.

References

1. http://www.osha.gov/OshDoc/data_General_Facts/ethylene-oxide-factsheet.pdf
2. http://en.wikipedia.org/wiki/Ethylene_oxide#cite_note-1
3. Lefort TE (1931) French Patent 729952
4. McClellan PP (1950) Ind Eng Chem 42:2402–2407
5. Kilty PA, Rol NC, Sachtler WMH (1973) Catal Lett 99:45–53
6. Geenen PV, Boss HJ, Pott GT (1982) J Catal 77:499–510
7. Iwakura G (1985) Japan Patent 63-126552
8. Tories N, Verikios XE (1987) J Catal 108:161–174
9. Bhasin MM (1988) US Patent 4,908,343
10. Matar S, Mirbach MJ, Tayim HA (1989) Catalysis in petrochemical processes. Kluwer Academic Publishers, Dordrecht, The Netherlands
11. Goncharova SN, Paukshtis EA, Bal'zhinimaev BS (1995) Appl Catal A: Gen 126:67–84
12. Kondaries DI, Verykios XE (1996) J Catal 158:363–377
13. Epling WS, Hoflund GB, Minahan DM (1997) J Catal 171:490–497
14. Jankowiak JT, Barteau MA (2005) J Catal 236:366–378
15. Amorim de Carvalho MCN, Passos FB, Schmal M (2007) J Catal 248:124–129
16. Law GH, Chitwood HC (1942) US Patent 2,279,470
17. Campbell CT, Paffett MT (1984) Appl Surf Sci 19:28–42
18. Tan SA, Grant RB, Lambert RM (1986) J Catal 100:383–391
19. Yeung KL, Gavriilidis A, Varma A, Bhasin MM (1998) J Catal 174:1–12
20. Jankowiak JT, Barteau MA (2005) J Catal 236:379–386
21. Suhr H, Pfreundschuh H (1988) Plasma Chem Plasma Process 8:67–74
22. Patiño P, Hernández FE, Rondón S (1995) Plasma Chem Plasma Process 15:159–171
23. Suhr H (1983) Plasma Chem Plasma Process 3:1–61
24. Zhou LM, Xue B, Kogelschatz U, Eliasson B (1998) Plasma Chem Plasma Process 18:375–393
25. Eliasson B, Hirth M, Kogeischatz U (1987) J Appl Phys 20:1421–1437

26. Chang MB, Tseng TD (1996) J Environ Eng 41–46
27. Orlandini I, Riedel U (2004) Catal Today 89:83–88
28. Magureanu M, Mandache NB, Parvulescu VI, Subrahmanyam Ch, Renken A, Kiwi-Minsker L (2007) Appl Catal B: Environ 74:270–277
29. Sarmiento B, Brey JJ, Viera IG, González-Elipe AR, Cotrino J, Rico VJ (2007) J Power Sources 169:140–143
30. Matin NS, Savadkoohi HA, Feizabadi SY (2008) Plasma Chem Plasma Process 28:189–202
31. Guo MX, Guo HC, Wang XS, Gong WM (2005) Chin J Chem 23:471–473
32. Chavadej S, Kiattubolpaiboon W, Rangsunvigit P, Sreethawong T (2007) J Mol Catal A: Chem 263:128–136
33. Chavadej S, Saktrakool K, Rangsunvigit P, Lobban LL, Sreethawong T (2007) Chem Eng J 132:345–353
34. Rueangjitt N, Sreethawong T, Chavadej S (2008) Plasma Chem Plasma Ptrocess 28:49–67
35. Sreethawong T, Thakonpatthanakun P, Chavadej S (2007) Int J Hydrogen Energ 32:1067–1079
36. Morinaga K, Suzuki M (1962) Bull Chem Soc Jpn 35:204–217
37. Supat K, Chavadej S, Lobban LL, Mallinson RG (2003) Ind Eng Chem Res 42:1654–1661
38. Supat K, Kruapong A, Chavadej S, Lobban LL, Mallinson RG (2003) Energ Fuel 17:474–481
39. Caldwell TA, Le H, Lobban LL, Mallinson RG (2001) Surface science and catalysis, vol 136. Elsevier, New York